

# Entropy generation and squeezing flow past a Riga plate with Cattaneo-Christov heat flux

M. ATLAS\*, S. HUSSAIN, and M. SAGHEER

Department of Mathematics, Capital University of Science and Technology, Islamabad, Pakistan

**Abstract.** In this article, we investigate the convective heat transfer of the two-dimensional unsteady squeezing flow past a Riga plate. To examine the heat transfer, Cattaneo-Christov heat flux model is used. Influence of entropy generation on heat transfer has been investigated numerically. With the help of suitable similarity transformation, the governing partial differential equations (PDEs) are converted into ordinary differential equations (ODEs). The obtained system of non-linear ordinary differential equations subject to the convective boundary conditions is solved by the shooting method using the computational software MATLAB. To strengthen the reliability of the results obtained by the shooting method, the MATLAB built-in function `bvp4c` has been used. The graphs show the effect of different physical parameters for velocity, temperature, concentration and tables are presented to observe the behaviour of skin friction and Sherwood number under the influence of certain physical parameters. It is observed that for increasing values of thermal relaxation parameter, the temperature profile increases and an opposite behaviour is shown for the concentration profile. Moreover, with an increase in the Brinkman number, the entropy generation increases.

**Key words:** squeezing flow, Riga plate, nanofluids, convective boundary conditions, Cattaneo-Christov heat flux, entropy generation.

## Nomenclature

$B$ – dimensionless constants	$Bi_1$ – Biot number for temperature	$b$ – width of magnets and electrodes
$C$ – concentration of fluid	$Re$ – Reynolds number	$\alpha$ – thermal diffusivity
$C_f$ – convective fluid concentration	$\chi$ – constant parameter	$\beta_R$ – mean observation constant
$C_h$ – ambient concentration	$Cf$ – skin friction coefficient	$S$ – squeezing parameter
$c_p$ – specific heat	$\phi$ – dimensionless concentration	$Rd$ – radiation parameter
$D_B$ – Brownian diffusion coefficient	$\lambda_1$ – constant parameter	$Sc$ – Schmidt number
$Be$ – Bejan number	$Sh_x$ – Sherwood number	$K_r$ – chemical reaction
$\rho_f$ – fluid density	$T$ – temperature of fluid	$B_r$ – Brinkman number
$M_0$ – magnetization	$T_h$ – ambient temperature	$\Omega$ – dimensionless temperature difference
$k$ – thermal conductivity	$(u, v)$ – velocity components	$Bi_2$ – Biot number for concentration
$\beta_e$ – relaxation time of heat transfer	$T_f$ – convective fluid temperature	$\eta$ – dimensionless variable
$\delta_e$ – Stefan Boltzman	$\pi$ – component of deformation	$\lambda_E$ – thermal radiation time
$Z$ – modified Hartman number	$V_f$ – fluid velocity	
$Pr$ – Prandtl number	$j_0$ – applied current density	

## 1. Introduction

The flow between two parallel plates or the flow in which the two boundaries approach each others is called the squeezing flow. Stefan [1] introduced the idea of squeezing flow by utilizing a lubrication conjecture. Squeezing flow has many applications not only in conventional engineering disciplines, but also in the modern and emerging areas of bio-engineering [2], chemical technology and pharmaceutical manufacturing [3], etc. Khaled and Vafai [4] studied the heat transfer and hydromagnetics effects of externally squeezed free stream over a horizontal surface. They concluded that both the local Nusselt

number and shear stress increase as the free stream velocity of squeezing increases. For unsteady flow Siddiqui et al. [5] extended the idea of Khaled and Vafai. Dib et al. [6] used the Duan-Rauch approach for unsteady squeezing nanofluid flow and obtained the solutions by using the differential transform method. Hayat et al. [7] solved mixed convection unsteady squeezing flow of three dimensional fluid by using the homotopy analysis method. MHD Squeezing flow in the presence of fractionalized nanofluid over a sensor surface was investigated by Haq et al. [8]. Later on, active and zero flux of nanoparticles between a squeezing channel presented by Atlas et al. [9]. More studies on squeezing flow can be found in [10–12].

To control the flow of an electrically conducting fluid over a flat plate, Gailitis and Lielausis [13] presented the idea to use Lorentz force. The flow control device named Riga plate consists of a spanwise aligned array of alternating electrodes and permanent magnets. It is an electromagnetic actuator. Pantokra-

\*e-mail: maleeha.atlas29@gmail.com

Manuscript submitted 2017-10-16, revised 2017-11-11, initially accepted for publication 2017-11-15, published in June 2018.

toras and Magyari [14] scrutinized the boundary layer flow of an electrically conducting fluid across a horizontal Riga plate. Sakiadis and Blasius flows for Riga plate were investigated by Pantokratoras [15] in 2011. In the existence of strong suction, mixed convection flow of a nanofluid past through a Riga plate was investigated by Ahmad et al. [16]. Hayat et al. [17] calculated the variable thickness originated by the nanofluid by using the homotopy analysis method. Ahmad et al. [18] studied the convective heat transfer of nanofluid flow past a vertical Riga plate. The shooting method was used to obtain the solution and it was found that the highest heat transfer rate is achieved in the absence of thermophoretic effect.

In many physical situations heat transfer occurring from one body to another is a natural process. Moving bodies are heated due to some external forces. The motion of bodies against other surfaces may also produce fractional heat which is of great interest. For example in highly efficient assembling machines, heat transfer analysis is very important. Heat transfer has many applications in biomedical, cooling of electronic devices and energy production. Heat transfer analyses are found in literature [19–24]. Recently, heat transfer analysis of MHD three dimensional flow in porous and deforming bodies are performed by Turkyilmazoglu [25]. In the first law of heat conduction, Fourier [26] analyzed the properties of heat transfer in 1822. Fourier’s law leads to a parabolic equation for the temperature field, though it is inadequate to express the features of heat transfer entirely. In every part of a material, any initial distraction is detected immediately. In practical terms, there is no such object or material that satisfies the Fourier law. The main shortcomings of the Fourier’s model were resolved by Cattaneo [27] by adding the partial time derivative in the constitutive relationship between the heat flux and temperature. The Cattaneo model introduced the time required to establish the steady heat conduction once a temperature gradient is imposed. This model is the hyperbolic energy equation and allows the transport of heat similar to the propagation of thermal waves having normal speed. Later on, Christov [28] presented the material invariant formulation of the Cattaneo’s model by introducing the Oldroyd’s upper-convected derivatives. Christov showed that without the convective derivative the Cattaneo model leads to a paradoxical evaluation of thermal waves in a moving frame. Ciarletta and Straughan theory [29] expressed the uniqueness and stability structure of the Cattaneo-Christov law. Han et al. [30] proposed the stretched flow of Maxwell fluid with Cattaneo-Christov model. Mustafa [31] examined the Cattaneo-Christov heat flux in the rotating flow of Maxwell nanofluid. Shah et al. [32] used shooting method to investigate Cattaneo-Christov heat flux in MHD flow of Maxwell fluid with Joule heating. Recently, Muhammad et al. [33] included the Cattaneo-Christov heat and mass flux in the squeezing flow.

Entropy generation has great importance due to its extensive involvement in heat exchangers, electronic cooling, turbo machinery, porous media and solar collectors. In many studies, first law of thermodynamics is the efficient way for the calculation of heat. In thermodynamics, diffusion, chemical reaction, friction force between solid surface and fluid viscosity within the system give rise to energy loss, which results in entropy gen-

eration in the system. Minimization of entropy generation was comprehensively covered by Bejan [34]. To modify the thermal engineering devices for higher thermal energy capacity, entropy generation minimization method has been used. Rashidi et al. [35] examined the MHD flow of nanofluid through a porous rotating disk and presented the results for entropy generation by utilizing the second law of thermodynamics. Butt and Ali [36] investigated analytically and numerically the effect of entropy generation on unsteady three dimensional squeezing flow. Entropy generation and mixed convection in a partially heated square cavity was numerically investigated by Hussain et al. [37]. Qing et al. [38] investigated the entropy generation on Casson nanofluid with MHD over a porous stretching/shrinking surface by using the successive linearization method and Chebyshev spectral collocation method.

In the present article, we discuss the unsteady two-dimensional squeezing flow between two Riga plates with the convective boundary conditions by using the Cattaneo-Christov heat flux model. The effect on entropy generation has also been discussed. Here, the governing partial differential equations of the model are converted to the ordinary differential equations by using the suitable similarity transformation. The approximate solution of resulting nonlinear coupled ODEs of such type of problems can be obtained using analytical techniques such as homotopy perturbation method [39], homotopy analysis method [40], optimal homotopy asymptotic method [41], differential transform method [42] and Adomian decomposition method [43] and some numerical techniques such as shooting method [23], etc. In [43], it was also discussed how to determine the correct range of physical parameters involved in the problem. For the proposed problem, we utilized the well-known shooting technique to obtain the solution of the reduced system of nonlinear ODEs together with the boundary conditions. The results are compared with those computed by the MATLAB built-in function `bvp4c` to the results obtained by the shooting method. Graphical and numerical results in the tabular form are shown for various values of the emerging parameters.

## 2. Problem formulation

We examine the squeezing flow of unsteady, viscous, incompressible two dimensional electromagnetohydrodynamic fluid flow between two Riga plates (see Fig. 1). The lower plate located at  $y = 0$  has the stretching velocity  $U_w = \frac{ax}{1-\gamma t}$  whereas the upper Riga plate is situated at  $y = h(t) = \sqrt{\frac{v_f(1-\gamma t)}{a}}$ . Fluid is squeezing with the velocity  $v_h = \frac{dh}{dt}$ . Heat flux through Cattaneo-Christov model [28] has been considered instead of heat flux in Fourier law of heat conduction. Here  $T_f$  and  $T_h$  denote the convective fluid and ambient temperature respectively. Variable temperature  $T_f = T_0 + d_1x$  and  $T_h = T_0 + d_2x$  at the plate and away from the plate, respectively, has been examined. Heat flux  $\mathbf{q}$  is taken as [33]

$$\mathbf{q} + \delta_E \left[ \frac{\partial \mathbf{q}}{\partial t} + \mathbf{V} \cdot \nabla \mathbf{q} + (\nabla \cdot \mathbf{V}) \mathbf{q} - \mathbf{q} \cdot \nabla \mathbf{V} \right] = -k \nabla T. \quad (1)$$

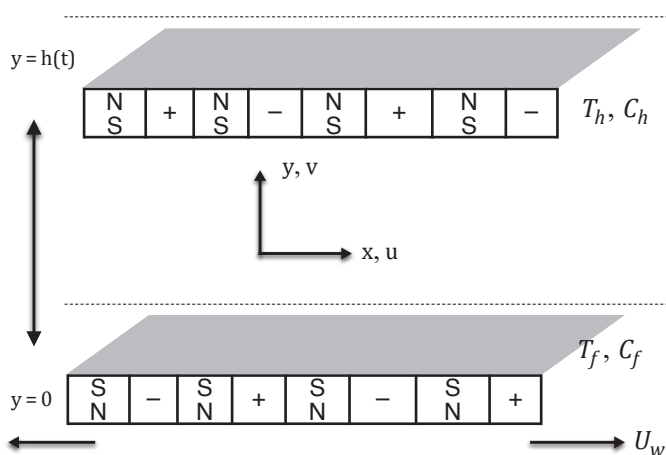


Fig. 1. Schematic diagram of the flow model

Here  $\mathbf{V}$ ,  $\delta_E$ , and  $k$  denote the velocity, relaxation time of heat flux and thermal conductivity of the fluid respectively. Classical Fourier's law is obtained from Eq. (1) when  $\delta_E = 0$ . Using the mass continuity equation  $\nabla \cdot \mathbf{V} = 0$ , the Eq. 1 reduces to the following form

$$\mathbf{q} + \delta_E \left[ \frac{\partial \mathbf{q}}{\partial t} + \mathbf{V} \cdot \nabla \mathbf{q} - \mathbf{q} \cdot \nabla \mathbf{V} \right] = -k \nabla T. \quad (2)$$

In the absence of viscous dissipation, the governing partial differential equations for velocity, temperature and concentration are given as follows [44]

$$\frac{\partial u}{\partial x} + \frac{\partial v}{\partial y} = 0, \quad (3)$$

$$\frac{\partial u}{\partial t} + u \frac{\partial u}{\partial x} + v \frac{\partial u}{\partial y} = \frac{1}{\rho_f} \frac{\partial p}{\partial x} + \nu_f \left( \frac{\partial^2 v}{\partial x^2} + \frac{\partial^2 v}{\partial y^2} \right) + \frac{\pi j_0 M_0 \text{Exp} \left( -\frac{\pi}{b} y \right)}{8 \rho_f}, \quad (4)$$

$$\frac{\partial v}{\partial t} + u \frac{\partial v}{\partial x} + v \frac{\partial v}{\partial y} = \frac{1}{\rho_f} \frac{\partial p}{\partial y} + \nu_f \left( \frac{\partial^2 v}{\partial x^2} + \frac{\partial^2 v}{\partial y^2} \right), \quad (5)$$

$$\frac{\partial T}{\partial t} + u \frac{\partial T}{\partial x} + v \frac{\partial T}{\partial y} + \lambda_E \Omega_E = \alpha \left( \frac{\partial^2 T}{\partial x^2} + \frac{\partial^2 T}{\partial y^2} \right) - \frac{1}{(\rho c_p)_f} \frac{\partial q_r}{\partial y}, \quad (6)$$

$$\frac{\partial C}{\partial t} + u \frac{\partial C}{\partial x} + v \frac{\partial C}{\partial y} = D_B \left( \frac{\partial^2 C}{\partial x^2} + \frac{\partial^2 C}{\partial y^2} \right) - K_1 (C - C_h). \quad (7)$$

subject to the boundary conditions

$$\left. \begin{aligned} y = 0 : u(x, y, t) &= \frac{ax}{1 - \gamma t}, v(x, y, t) = 0, \\ -k \frac{\partial T}{\partial y} &= h_1 (T_f - T), -D \frac{\partial C}{\partial y} = h_2 (C_f - C), \\ y = h(t) : u(x, y, t) &= 0, v(x, y, t) = v_h = \frac{dh}{dt}, \\ T &= T_h, C = C_h. \end{aligned} \right\} \quad (8)$$

The boundary conditions describe that the lower plate is placed at  $y = 0$  and stretched in the  $x$ -direction with the velocity  $U_w = \frac{ax}{1 - \gamma t}$  and in the  $y$ -direction with the velocity  $v = 0$  [44]. We establish the convective boundary conditions at the lower surface for temperature and concentration [45]. The convective boundary conditions described the energy balance at the fluid-solid interface. At the upper plate the velocity in the  $x$ -direction is zero and the velocity in the  $y$ -direction is the squeezing time dependent velocity of fluid. The Dirichlet boundary conditions are used for temperature and concentration at the upper plate. In (6)  $\Omega_E$  is formulated as [33]

$$\begin{aligned} \Omega_E = & \frac{\partial^2 T}{\partial t^2} + u \frac{\partial u}{\partial x} \frac{\partial T}{\partial x} + v \frac{\partial v}{\partial y} \frac{\partial T}{\partial y} + u^2 \frac{\partial^2 T}{\partial x^2} + \\ & + v^2 \frac{\partial^2 T}{\partial y^2} + \frac{\partial u}{\partial t} \frac{\partial T}{\partial x} + 2uv \frac{\partial^2 T}{\partial x \partial y} + 2u \frac{\partial^2 T}{\partial x \partial t} + \\ & + u \frac{\partial v}{\partial x} \frac{\partial T}{\partial y} + \frac{\partial v}{\partial t} \frac{\partial T}{\partial y} + v \frac{\partial u}{\partial y} \frac{\partial T}{\partial x} + 2v \frac{\partial^2 T}{\partial y \partial t}. \end{aligned} \quad (9)$$

According to the Rosseland approximation [9] the thermal radiation heat flux considered as

$$q_r = \frac{-4\delta_e}{3\beta_R} \frac{\partial T^4}{\partial y}, \quad (10)$$

where  $\delta_e$  is the Stefan Boltzman constant and  $\beta_R$  the mean observation constant. We expand  $T^4$  by using the Taylor series about temperature  $T_h$  to have

$$T^4 = 4T_h^3 - T_h^4. \quad (11)$$

The following local similarity transformations [44] have been introduced to convert (3-7) into nondimensional form:

$$\begin{aligned} \Psi &= \sqrt{\frac{av_f}{1 - \gamma t}} x f(\eta), \quad \theta(\eta) = \frac{T - T_f}{T_h - T_f}, \\ u &= \frac{\partial \Psi}{\partial y} = U_w f'(\eta) \\ v &= -\frac{\partial \Psi}{\partial x} = -\sqrt{\frac{av_f}{1 - \gamma t}} f(\eta), \quad \eta = \frac{y}{h(t)}, \\ \phi(\eta) &= \frac{C - C_f}{C_h - C_f}. \end{aligned} \quad (12)$$

Eq. (3) is identically satisfied and (4–7) get the following form

$$f'''' + ff''' - f'f'' - \frac{S}{2}(3f'' + \eta f''') - ZBe^{-B\eta} = 0, \quad (13)$$

$$(1 + Rd)\theta'' + Pr(f\theta' + \frac{\eta}{2} S\theta') - Pr\beta_e(ff'\theta' + f^2\theta'' - S\eta f\theta'') - \frac{Pr}{4}\beta_e S^2(3\eta\theta' + \eta^2\theta'') + \frac{Pr}{2}S\beta_e(\eta f'\theta' + 3f\theta') = 0, \quad (14)$$

$$\phi'' + Sc\left(f\phi' - \frac{S}{2}\eta\phi' - K_r\phi\right) = 0. \quad (15)$$

By applying the similarity transformation (12) to (8) the boundary conditions get the following form:

$$\left. \begin{aligned} \eta = 0 : f(\eta) = 0, f'(\eta) = 1, \theta'(\eta) = -Bi_1(1 - \theta(\eta)), \\ \phi'(\eta) = -Bi_2(1 - \phi(\eta)), \\ \eta = 1 : f(\eta) = \frac{S}{2}, f'(\eta) = 1, \theta(\eta) = 0, \phi(\eta) = 0. \end{aligned} \right\} \quad (16)$$

Different dimensionless parameters appearing in (13–16) are defined as

$$S = \frac{\gamma}{a}, \quad B = \frac{\pi h(t)}{b}, \quad Z = \frac{\pi_j M_0 x}{8\rho_f U_w^2}, \quad Rd = \frac{16T_h^3 \sigma_e}{3\beta_R k},$$

$$Pr = \frac{\nu}{\alpha}, \quad K_r = \frac{k_1(1 - \gamma t)}{a}, \quad Sc = \frac{\nu}{D_B},$$

$$Bi_1 = \frac{-h_1}{k} \sqrt{\frac{\nu_f(1 - \gamma t)}{a}}, \quad Bi_2 = \frac{-h_2}{k} \sqrt{\frac{\nu_f(1 - \gamma t)}{a}}.$$

The important physical parameters of interest, skin friction coefficient and Sherwood number, are formulated as follows.

$$Cf = \frac{\tau_w}{\rho_f U_w^2}, \quad Sh_x = \frac{xq_m}{D(C_f - C_h)},$$

where  $\tau_w$  is the skin friction or shear stress and  $q_m$  the concentration flux from the surface and are given by

$$\tau_w = \mu_f \left( \frac{\partial u}{\partial y} \right)_{y=h(t)}, \quad q_m = -D \left( \frac{\partial C}{\partial y} \right)_{y=h(t)}.$$

Dimensionless forms of skin friction, and Sherwood number are

$$Cf Re_x^{1/2} = -f''(1), \quad Sh_x Re_x^{-1/2} = -\phi'(1).$$

The entropy generation of the nanofluid is given by [46]

$$S_{gen}''' = \frac{k}{T_\infty^2} \left[ \left( \frac{\partial T}{\partial y} \right)^2 + \frac{16\sigma_T^3}{T_\infty^2} \left( \frac{\partial T}{\partial y} \right)^2 \right] + \frac{\mu}{T_\infty} \left( \frac{\partial u}{\partial y} \right)^2 + \frac{R_D}{C_\infty} \left( \frac{\partial C}{\partial y} \right) + \frac{R_D}{T_\infty} \left( \frac{\partial T}{\partial y} \frac{\partial C}{\partial y} \right).$$

In the above equation, the first term is due to heat transfer (also known as heat transfer irreversibility HTI), second term is due to fluid friction (also known that fluid friction irreversibility FFI) and third term is due to mass transfer (also known as the mass transfer irreversibility MTI). The characteristic entropy generation is defined as

$$S_0''' = \frac{k(\nabla T)^2}{L^2 T_\infty^2}. \quad (17)$$

By using the similarity transformation, the entropy generation in the dimensionless form can be written as

$$N_G = \frac{S_{gen}'''}{S_0'''} = Re(1 + Rd)\theta'^2(\eta) + \frac{ReBr}{\Omega} f''^2(\eta) + Re\lambda_1 \left( \frac{\chi}{\Omega} \right)^2 \phi'^2(\eta) + Re\lambda_1 \left( \frac{\chi}{\Omega} \right)^2 \theta'(\eta) \phi'(\eta),$$

where

$$Re = \frac{\mu_f L^2}{\nu}, \quad Br = \frac{\mu U_w^2}{k\Delta T}, \quad \Omega = \frac{\Delta T}{T_\infty}, \quad \chi = \frac{\Delta C}{C_\infty}, \quad \lambda_1 = \frac{R_D C_\infty}{k}.$$

Another dimensionless parameter is considered which is the Bejan number [47]. It is the ratio of the entropy generation due to heat and mass transfer irreversibility to the total entropy generation given by

$$Be = \frac{HTI + MTI}{N_G}.$$

### 3. Solution methodology

The system of non-linear ordinary differential equations (13–15) subject to the boundary conditions (16) has been solved numerically by the shooting method [48] for different values of governing parameters. We denote  $f \rightarrow f_1, f_1' \rightarrow f_2, f_2' \rightarrow f_3, f_3' \rightarrow f_4, \theta \rightarrow f_5, \theta' \rightarrow f_6, \phi \rightarrow f_7$  and  $\phi' \rightarrow f_8$ . The boundary value problem (13–17) are converted to 8 first order differential equations of the initial value problem.

$$\begin{aligned} f_1' &= f_2, \\ f_2' &= f_3, \\ f_3' &= f_4, \\ f_4' &= f_2 f_3 - f_1 f_4 + \frac{S}{2}(3f_3 + \eta f_4) + ZBe^{-B\eta}, \\ f_5' &= f_6, \end{aligned}$$

$$f_6' = \frac{Pr \left[ \left( \frac{S}{2} \eta f_6 - f_1 f_6 \right) - \beta_e \left( \frac{3}{4} S^2 \eta f_6 + f_1 f_2 f_6 + \frac{S}{2} \eta f_2 f_6 + \frac{3}{2} S f_1 f_6 \right) \right]}{1 + Rd - \frac{1}{4} Pr \beta_e S^2 \eta^2 - Pr f_1^2 \beta_e + Pr S \beta_e \eta f_1}$$

$$\begin{aligned} f_7' &= f_8, \\ f_8' &= -Sc \left[ f_1 f_8 - \frac{S}{2} \eta f_8 + K_r f_7 \right]. \end{aligned}$$

subject to the initial conditions

$$\begin{aligned} f_1(0) &= 0, f_2(0) = 1, f_3(0) = p, \\ f_4(0) &= q, f_5(0) = r, \\ f_6(0) &= -Bi_1(1 - f_5(0)), f_7(0) = t, \\ f_8(0) &= -Bi_2(1 - f_7(0)). \end{aligned} \tag{18}$$

We solve the above initial value problem by the RK4 method by choosing some appropriate values for  $p, q, r$  and  $t$ . For the refinement of  $p, q, r$  and  $t$ , we apply the Newton's method until we meet the following convergence criteria:

$$\max \left\{ \left| f_1(1) - \frac{S}{2} \right|, \left| f_2(1) \right|, \left| f_3(1) \right|, \left| f_7(1) \right| \right\} < \varepsilon,$$

where  $\varepsilon > 0$  is a small positive real number. All the numerical results in this paper are achieved with  $\varepsilon = 10^{-6}$ .

To validate our code by the shooting method, we have computed the numerical results by the MATLAB built-in function bvp4c. For further reliability of our results, we reproduce the skin friction coefficient reported by Hayat et al. [44]. The comparison presented in Table 1 indicates a strong agreement between our results and those of Hayat et al. For this comparison we have chosen  $\beta_e = 0, K_r = 0.2, Sc = 0.5, Bi_1 = 0.2 = Bi_2, Pr = 1.5$ .

Table 1  
Comparison of the skin friction coefficient  $CfRe_x^{1/2}$

S	Z	Present results		Hayat [44]	
		Shooting	bvp4c	HAM	Numerical
0.1	1.5	1.69643	1.69643	1.69635	1.69634
0.3		1.08549	1.08549	1.08543	1.08543
0.5		0.46756	0.46756	0.46751	0.46751
0.5	0.0	0.42215	0.42215	0.42215	0.42215
	1.0	0.45243	0.45243	0.45239	0.45239
	1.5	0.46756	0.46756	0.46751	0.46751

Table 2

Numerical values of  $Sh_x Re_x^{-1/2}$  when  $\beta_e = 0.1, B = 10.0, Bi_1 = 0.2 = Bi_2, Z = 1.5, S = 0.2, Pr = 1.5$

Sc	$K_r$	$Sh_x Re_x^{-1/2}$	
		Shooting	bvp4c
1.0	0.2	0.16598	0.16598
2.0		0.14395	0.14395
3.0		0.12571	0.12571
4.0		0.11044	0.11044
4.0	0.3	0.17513	0.17513
	0.5	0.16825	0.16825
	1.0	0.15288	0.15288
	1.2	0.14737	0.14737

#### 4. Results and discussion

In this section, we examine the numerical solution of the mathematical model (13–16) for different choices of the values of some important physical parameters. We first present the numerical results of some parameters of interest in the form of tables followed by the discussion on the graphical behaviour of certain important profiles.

Table 2 describes the effect of chemical reaction parameter  $K_r$  and Schmidt number  $Sc$  on the Sherwood number. It can be seen from the table that as the values of chemical reaction  $K_r$  increase, the Sherwood number exhibits the decreasing behaviour and the increasing values of Schmidt number  $Sc$  also show that the Sherwood number decreases. Figure 2 shows the effect of positive and negative values of squeezing parameter  $S$  on the velocity profile. For increasing values of positive squeezing parameter, the velocity profile increases. The graph exhibits that as the upper plate moves towards the lower plate that causes a force which provides more velocity to

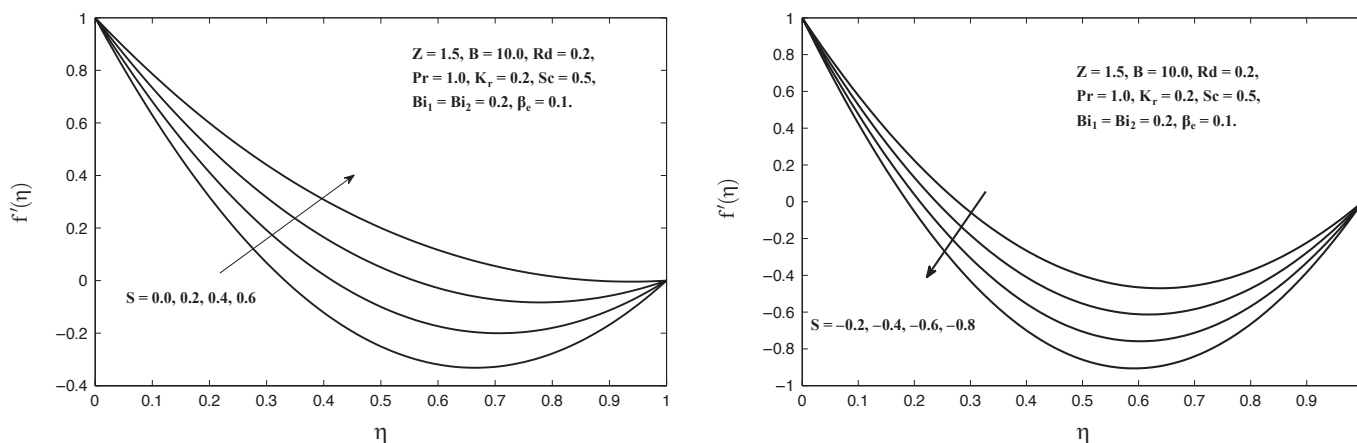


Fig. 2. Influence of  $S$  on  $f'$

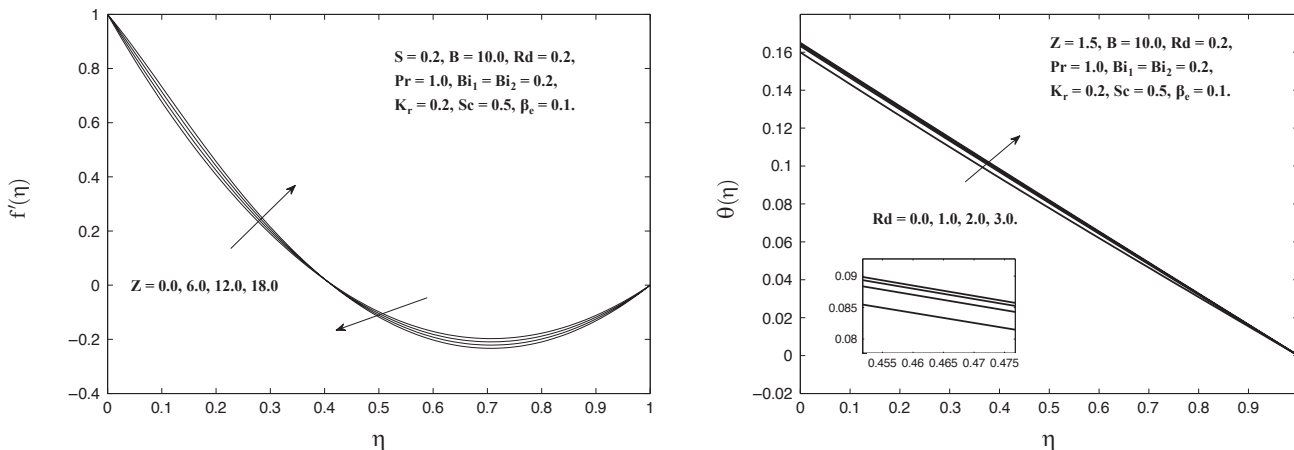


Fig. 3. Influence of  $Z$  on  $f'$  and  $Rd$  on  $\theta$

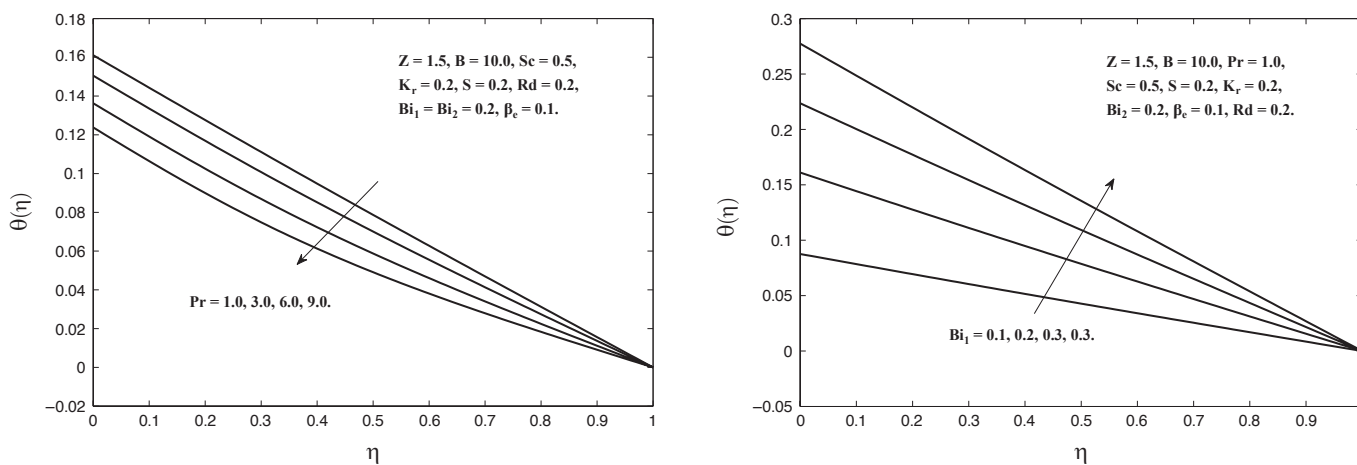


Fig. 4. Influence of  $Pr$  and  $Bi_1$  on  $\theta$

the motion of fluid. The negative values of squeezing parameter  $S$  on the velocity profile shown that for decreasing values of squeezing parameter the velocity graph decreases. It can be concluded that the graph decreases due to the motion of the upper plate away from the lower plate. As a result, vacuum is created in the middle of the channel. To fill this gap, fluid starts moving in the upward direction, which results the decrease of the velocity profile. Figure 3 exhibits the effect of modified Hartman number  $Z$  on the velocity profile and the effect of thermal radiation parameter  $Rd$  on the temperature profile. As the values of Hartman number increase, the fluid velocity increases near the lower plate, whereas the velocity near the upper plate decreases. Physically, increasing values of modified Hartman number correspond to high intensity of external electric field, which is responsible for the production of Lorentz force parallel to wall. It can be observed that the temperature profile increases as the value of radiation parameter increases.

Figure 4 shows the effect of Prandtl number  $Pr$  and Biot number  $Bi_1$  on the temperature profile. Prandtl number represents the ratio of the momentum diffusivity to heat diffusivity. It can be can be observed that for large  $Pr$

temperature profile decreases. The increasing values of Prandtl number make convection dominate in transferring energy from the channel, whereas the case of conduction is opposite in nature. It can be exhibits from the figure that for increasing values of Biot number the temperature profile increases. Physically, temperature versus thermal Biot number reflect the interaction between conduction in solid and convection at its surface. The increasing values of Biot number for temperature result in an enhancement of temperature profile. As the value of Biot number increases, there is reduction in the thermal resistance of the surface. Due to an increase in convection, higher surface temperature is attained. Figure 5 shows the influence of squeezing parameter  $S$  and temperature relaxation parameter  $\beta_e$  on the temperature profile. As the value of squeezing parameter increases the temperature profile decreases. It can be visualized from the figure that for increasing values of thermal relaxation parameter the temperature profile decreases. As the values of thermal relaxation parameter increases, the fluid particles need more time for transferring heat to the adjoining particles, which results in the fall of the temperature profile.

Figure 6 exhibits the effect of Schmidt number  $Sc$  and Biot number  $Bi_2$  on the concentration profile. For increasing

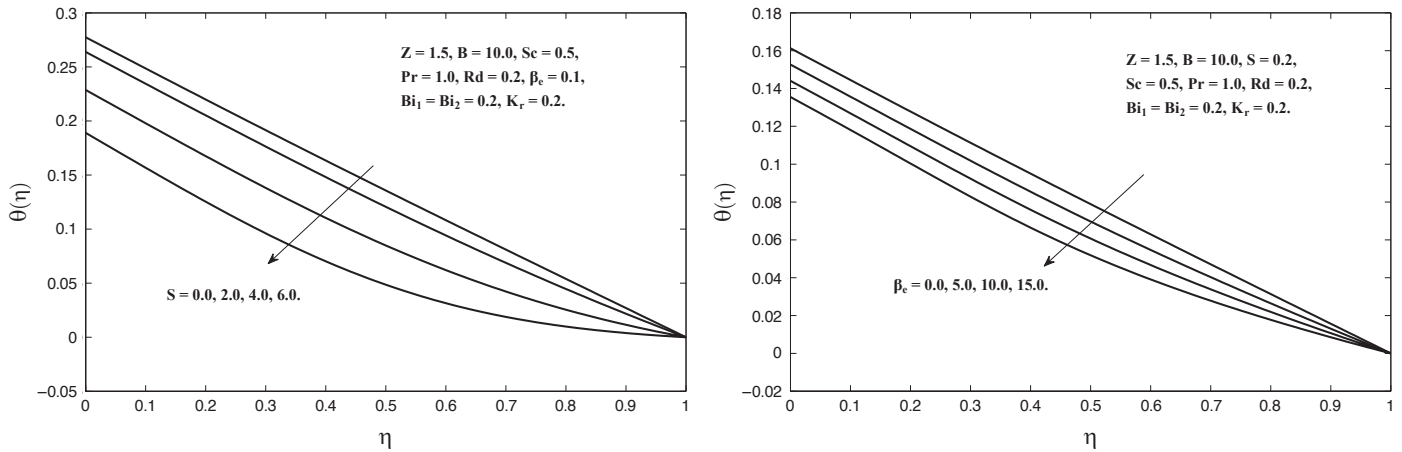


Fig. 5. Influence of  $S$  and  $\beta_e$  on  $\theta$

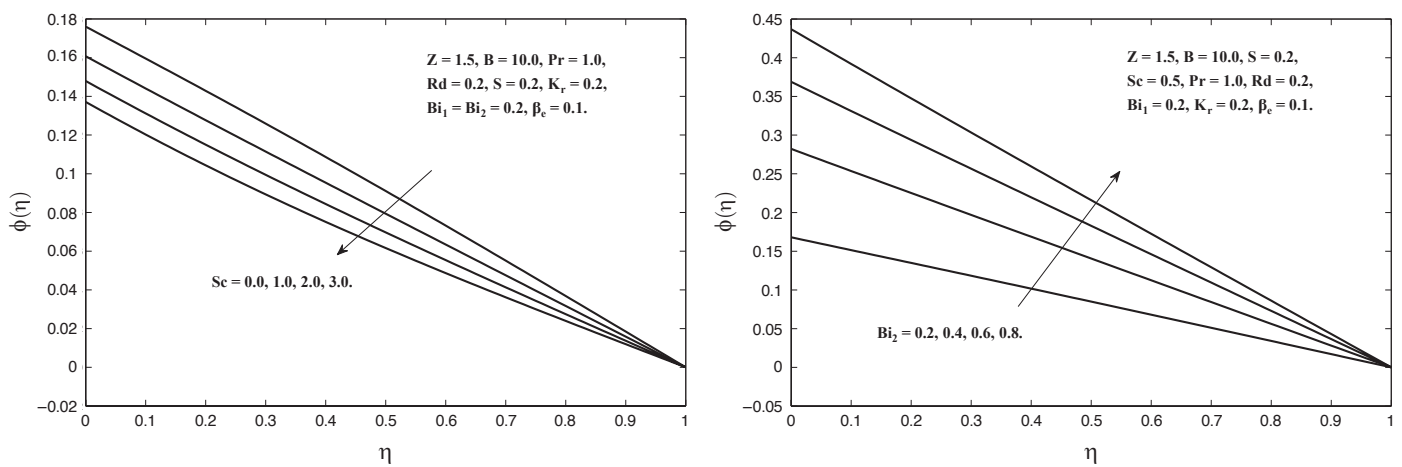


Fig. 6. Influence of  $Sc$  and  $Bi_2$  on  $\phi$

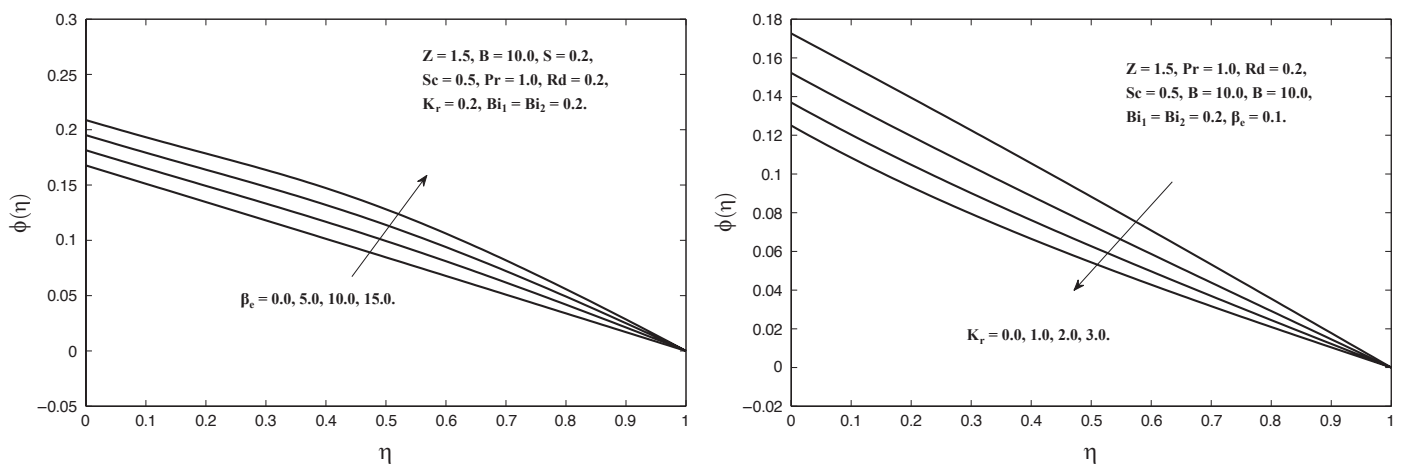


Fig. 7. Influence of  $Sc$  and  $Bi_2$  on  $\phi$

values of Schmidt number, the concentration profile decreases. Schmidt number is the ratio of momentum diffusivity to the mass diffusivity, so larger value of Schmidt number is expected to cause less mass diffusivity. As a result concentration profile decreases. For increasing values of Biot number  $Bi_2$  for

concentration, the concentration profile increases. This rise is linked to higher values of Biot number, which indicate a deeper penetration of concentration. Figure 7 exhibits the influence of relaxation parameter  $\beta_e$  and chemical reaction parameter  $K_r$  on the concentration profile. For increasing values

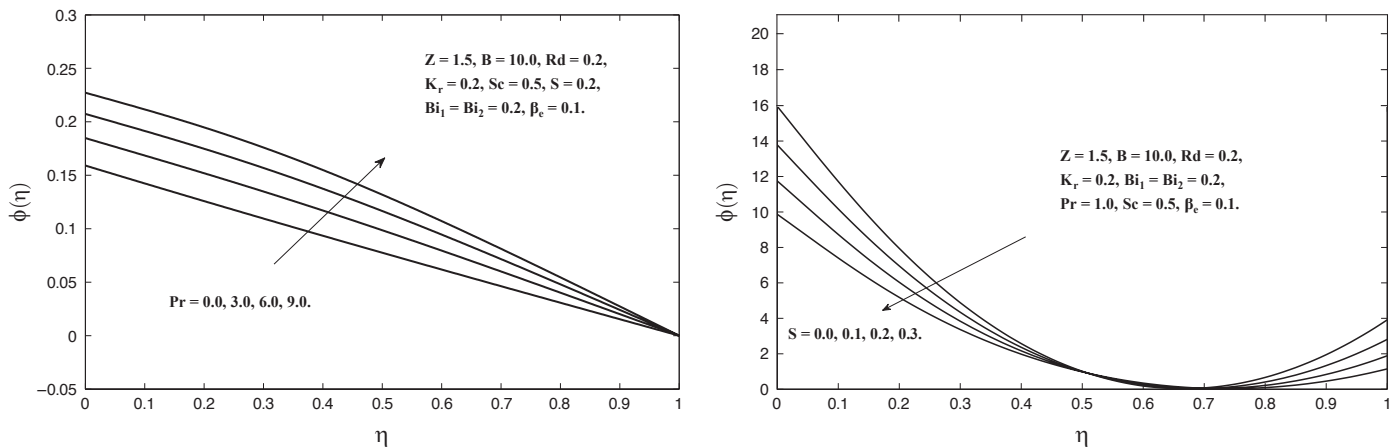


Fig. 8. Influence of  $Pr$  on  $\phi$  and  $S$  on  $N_G$

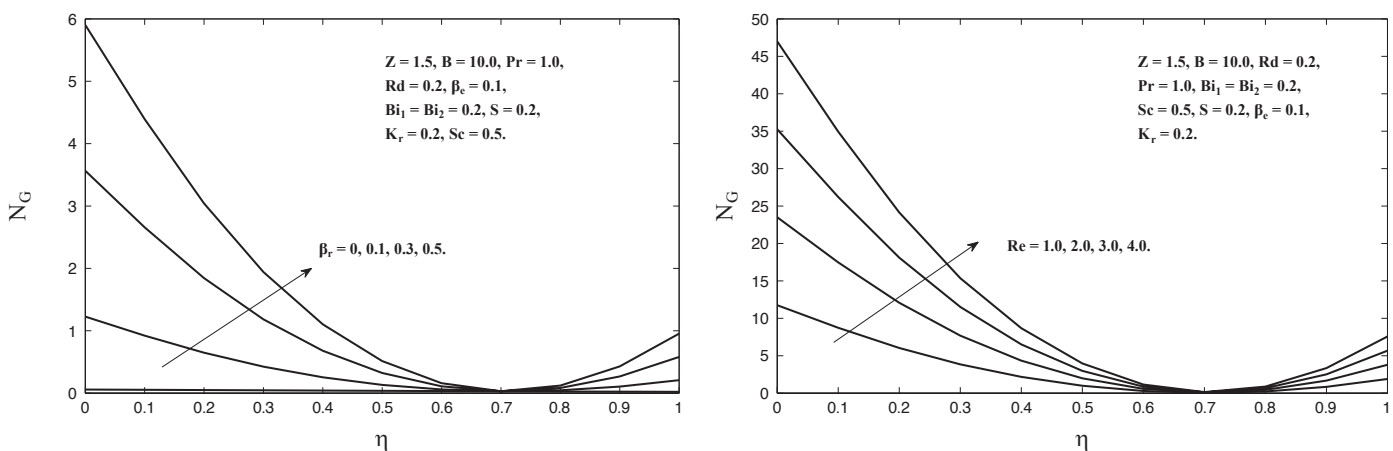


Fig. 9. Influence of  $\beta_r$  and  $Re$  on  $N_G$

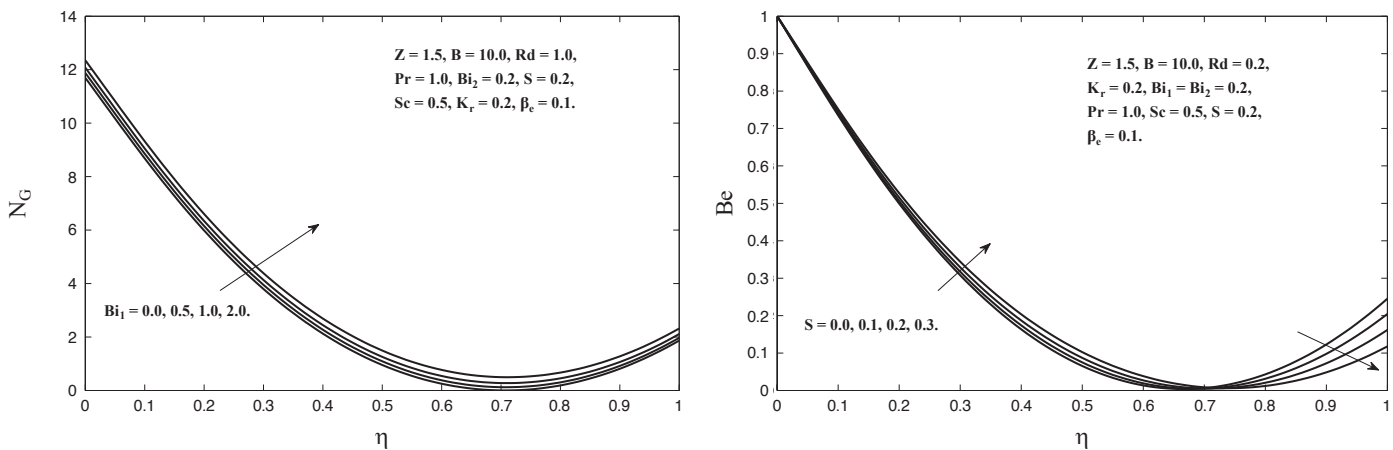
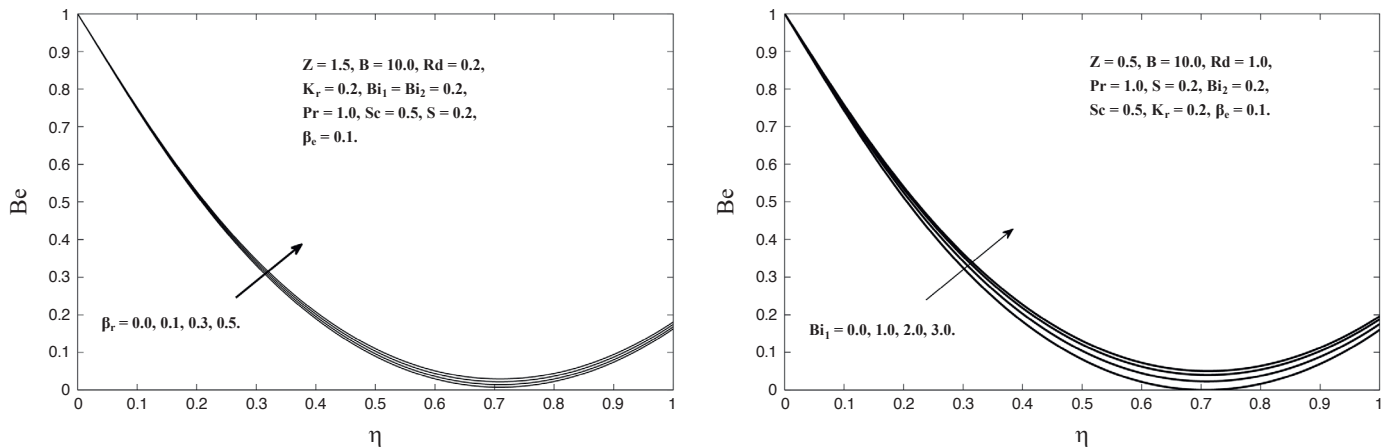


Fig. 10. Influence of  $Bi_1$  on  $N_G$  and  $S$  on  $Be$

of relaxation parameter, the concentration profile increases. For increasing values of chemical reaction the concentration profile decreases, because the increasing values of chemical reaction result a reduction in the molecular diffusivity. Figure 8 shows the influence of prandtl number  $Pr$  on concentration

profile. For increasing values of Prandtl, the boundary layer thickness increases.

Figures 8–11 show the effect of different parameters on entropy generation for  $Re = 0.1$ ,  $\Omega = 1.0$ ,  $\chi = 0.2$ ,  $\lambda_1 = 0.2$  and  $\beta_r = 1.0$ . Figure 8 shows the effect of squeezing param-

Fig. 11. Influence of  $\beta_r$  and  $Bi_1$  on  $Be$ 

eter  $S$  on entropy generation  $N_G$ . It can be concluded from this figure that due to increase in squeezing parameter, the entropy generation number  $N_G$  decreases. The entropy is more prominent near the walls of the channel than at the center. Figure 9 shows the effect of Brinkman number  $\beta_r$  and  $Re$  on the entropy profile  $N_G$ . For increasing values of Brinkman number, the entropy generation  $N_G$  increases. The increase in the entropy is produced by the irreversibility of fluid friction. As  $Re$  increases the entropy generation parameter  $N_G$  increases. From the figure, it can be observed that there is more disturbance in the movement of the fluid and there is an increase in the entropy generation due to the contribution of fluid friction and heat transfer. Figure 10 exhibits the effect of Biot number for temperature  $Bi_1$  on entropy generation  $N_G$  and squeezing parameter  $S$ . It can be observed that for increasing values of Biot number the entropy profile increases on Bejan number  $Be$ . For increasing values of  $S$  the graph of  $Be$  increases. It can be observed that near the lower wall of the channel, the graphs are confined in the region  $0 < Be < 0.7$ , which suggests that fluid friction entropy is dominant; in fact, entropy due to heat and mass transfer is dominant. Figure 11 shows the effect of Brinkman number  $\beta_r$  and Biot number  $Bi_1$  on  $Be$ ; for increasing values of  $\beta_r$ , the profile of  $Be$  increases. For increasing values of  $Bi_1$  the profile of  $Be$  increases.

## 5. Conclusions

In the presence of magnetic field, squeezing flow between two Riga plates is investigated numerically. Cattaneo-Christov model is incorporated for heat transfer. The ordinary differential equations along with the boundary conditions were solved numerically with the shooting method and the results are compare with Matlab built-in function bvp4c. The main findings of the article are as follows.

- Velocity profile increases for increasing values of the squeezing parameter  $S$  and decreases for decreasing values of  $S$ .

- A little enhancement in temperature is observed for increasing values of thermal radiation  $Rd$  and temperature profile decreases for increasing values of thermal relaxation parameter  $\beta_e$ .
- Concentration profile decreases for increasing values of chemical reaction parameter  $K_r$ .
- Entropy generation has decreasing behaviour for increasing values of squeezing parameter  $S$  and increasing behaviour is observed for increasing values of mean observation constant  $\beta_r$ .
- Bejan number  $Be$  demonstrated that fluid friction impact are stronger near the lower stretching wall and heat and mass transfer effect are prominent in the upper wall.

## REFERENCES

- [1] M.J. Stefan, "Versuch Uber die scheinbare uhdesion, Akad. wiss. weinmath", *Math-Nat Wiss Ki.* 69, 713–721 (1874).
- [2] J. Engmann, C. Servais, and A. S. Burbidge, "Squeeze flow theory and applications to rehomety: A review", *N. New. F. Mech.* 132, 01–27 (2005).
- [3] X. Chunhui, L. Yuan, X. Yong, and W. Hang, "Squeeze flow of interstitial Herschel-Bulkely fluid flow between two rigid spheres", *Particuology* 8, 360–364 (2010).
- [4] A.R.A. Khaled, and K. Vafai, "Hydromagnetic squeezed flow and heat transfer over a sensor surface", *Int. J. Eng. Sci.* 42, 509–519 (2004).
- [5] A.M. Siddiqui, S. Irrum, and A.R. Ansari, "Unsteady squeezing flow of a viscous MHD fluid between parallel plates", *Math. Model. Anal.* 13, 565–576 (2008).
- [6] A. Dib, A. Haiahem, and B.B. Said, "Approximate analytical solution of squeezing unsteady nano-fluid flow", *Powder. Technol.* 269, 193–199 (2014).
- [7] T. Hayat, A. Qayyum, and A. Alsaedi, "Three dimensional mixed convection squeezing flow", *Appl. Math. Mec.* 36, 47-60 (2015).
- [8] R.U. Haq, S. Nadeem, Z.H. Khan, and N.F. Noor, "MHD squeezed flow of water functionalized metallic nanoparticles over a sensor surface", *Phys. E* 73, 45–53 (2015).
- [9] M. Atlas, R.U. Haq, and M. Mekkaoui, "Active and Zero flux of nanoparticles between a squeezing channel with thermal radiation effects", *J. Mol. Liq.* 223, 289–298 (2016).

- [10] M. Sheikholeslami, and D.D. Ganji, "Effect of adding nanoparticle on squeezing flow and heat transfer improving using KKL method", *Int. J. Numer. Methods Fluid* 27, 1535–1553 (2017).
- [11] M. Khan and M. Azam, "Unsteady heat and mass transfer mechanism in MHD Carreau nanofluid flow", *J. Mol. Liq.* 225, 554–562 (2017).
- [12] A.S. Dagonchi and D.D. Ganji, "Analytic solution and heat transfer of two phase nanofluid flow between two parallel walls considering Jouel heating effects", *J. Mol. Liq.* 318, 390–400 (2017).
- [13] A. Gailitis and O. Lielausis, "On a possibility to reduce the hydrodynamics resistance of a plate in an electrolyte", *Appl. Magnet. Rep. Phy. Inst.* 12, 143–146 (1961).
- [14] A. Pantokrators and E. Magyari, "EMHD free convection boundary layer flow from a Riga plate", *J. Eng. Math.* 64, 303–315 (2009).
- [15] A. Pantokrators, "The Blasius and Sakiadis flow along a Rigaplate", *Prog. Comput. Fluid. Dy.* 11(5), 329–333 (2011).
- [16] A. Ahmad, S. Asghar and S. Afzal, "Flow of a nanofluid past a Riga plate", *J. Magn. Magn. Mater.* 402, 44–48 (2016).
- [17] T. Hayat, T. Abbas, M. Ayub, M. Farooq, and A. Alsaedi, "Flow of nanofluid due to convectively heated Riga plate with variable thickness", *J. Mol. Liq.* 222, 854–862 (2016).
- [18] R. Ahmad, M. Mustafa, and M. Turkyilmazoglu, "Buoyancy effects on nanofluid flow past a convectively heated Riga plate.", *Int. J Heat Mass Trans* 111, 827–835 (2017).
- [19] M. Sheikholeslami and D.D. Ganji, "Numerical investigation of nanofluid melting heat transfer between two pipes", *Alex. Eng. J.* (2017).
- [20] N. Bozorgan and M. Shafahi, "Analysis of Gasketed plate heat exchanger performance using nanofluid", *J. Heat Mass Trans. Research* (2017).
- [21] E. Abu-Nada, "Simulation of heat transfer enhancement in nanofluids using dissipative particle dynamics", *Int. Commu. Heat Mass Trans.* 85, 1–11 (2017).
- [22] M. Sheikholeslami, and M.M. Bhatti, "Active method for nanofluid heat transfer enhancement by means of EHD", *Int. J. Heat Mass Trans* (2017).
- [23] M. Bilal, S. Hussain, and M. Sagheer, "Boundary layer flow of magneto-micropolar nanofluid flow with Hall and ion-slip effects using variable thermal diffusivity", *Bull. Pol. Ac.: Tech.* 65(3), 383–390 (2017).
- [24] A. Rauf, S.A. Shehzad, T. Hayat, M.A. Meraj, and A. Alsaedi, "MHD stagnation point flow of micro nanofluid towards a shrinking sheet with convective and zero mass flux conditions", *Bull. Pol. Ac.: Tech.* 65(2), 155–162 (2017).
- [25] M. Turkyilmazoglu, "Equivalences and correspondences between the deforming body induced flow and heat in three dimension", *Phys. Fluid* 28, 043–102 (2016).
- [26] J.B.J. Fourier, *Theorie Analytique De La Chaleur*, Chez Firmin Didot, Paris, 1822.
- [27] C. Cattaneo, "Sulla conduzione del calore Atti semin", *Mat. Fis. Univ. Modena Reggio Emilia* 5, 83–101 (2009).
- [28] C.I. Christov, "On frame indifferent formulation of the Maxwell-Cattaneo model of finite speed heat conduction", *Mech. Res. Commun.* 36, 481–486 (2009).
- [29] M. Ciarletta and B. Straughan, "Unique and structural stability for the Cattaneo-Christov equations", *Mech. Res. Commun.* 37, 445–447 (2010).
- [30] S. Han, L. Zheng, C. Li, and X. Zhang, "Coupled flow and heat transfer in viscoelastic fluid with Cattaneo-Christov heat flux model", *Appl. Math. Lett.* 38, 87–93 (2014).
- [31] M. Mustafa, "Cattaneo-Christov heat flux model for rotating flow and heat transfer of upper-convective maxwell nanofluid", *AIP Adv.* 5, 47–109 (2015).
- [32] S. Shah, S. Hussain, and S. Sagheer, "MHD effects and heat transfer for the UCM fluid along with Jouel heating and thermal radiation using Cattaneo-Christov heat flux model", *AIP Adv.* 6 (2016).
- [33] N. Muhammad, S. Nadeem, and T. Mustafa, "Squeezed flow of a nanofluid with Cattaneo-Christov heat and mass fluxes", *Res. Phys.* 7 (2017).
- [34] A. Bejan, "Entropy generation minimization: The new Thermodynamic of finite size devices and finite time process", *J. Appl. phys.* 79 (1996).
- [35] M.M. Rashidi, S. Abelman, and N. Freidoonimehr, "Entropy generation in steady MHD flow due to rotating porous disk in nanofluid", *Int. J. Heat Mass Transfer.* 62, 515–525 (2013).
- [36] A.S. Butt and A. Ali, "Analysis of entropy generation effects in unsteady squeezing flow in a rotating channel with lower stretching permeable wall", *J. Taiwan Inst. Chem. Eng.* 48, 8–17 (2015).
- [37] S. Hussain, K. Mehmood, and M. Sagheer, "MHD mixed convection and entropy generation of water-alumina nanofluid flow in a doubled lid driven cavity with discrete heating", *J. Magn. Magn. Mater* 419, 140–155 (2016).
- [38] J. Qing, M.M. Bhatti, M.A. Abbas, M.M. Rashidi, and M.E.S. Ali, "Entropy generation on MHD Casson nanofluid flow over a porous stretching/shrinking surface", *Entropy* 18, 123 (2016).
- [39] J.H. He, "Homotopy perturbation technique", *Comput. Methods Appl. Mech. Eng.* 178(3), 257–262 (1999).
- [40] O.A. Béq, M.M. Rashidiand, A.T. Béq, and M. Asadi, "Homotopy analysis of transient magneto-bio-fluid dynamics of micropolar squeeze film in a porous medium: a model for magneto-bio-rheological lubrication", *J. Mech. Medi. Bio.* 12(3), 125–151 (2012).
- [41] M. Qayyum, H. Khan, and M.T. Rahim, "A novel approach to approximate unsteady squeezing flow through porous medium.", *J. Prime Res. Math.* 12 (2016).
- [42] A.S. Dogonchiand, M. Hatami, K.H. Hosseinzadeh, and G. Domairry, "Non-spherical particles sedimentation in an incompressible Newtonian medium by Padé approximation", *Powder Tech.* 278, 248–256 (2015).
- [43] M. Turkyilmazoglu, "Determination of the correct range of physical parameters in the approximate analytical solutions of nonlinear equations using the Adomian decomposition method", *Mediterr. J. Math.* 13(6), 4019–4037 (2016).
- [44] T. Hayat, M. Khan, M. Imtiaz, and A. Alsaedi, "Squeezing flow past a Riga plate with chemical reaction and convective conditions", *J. Mol. Liq.* 225, 569–576 (2016).
- [45] T. Hayat, K. Muhammad, Khursheed, M. Farooq, and A. Alsaedi, "Unsteady squeezing flow of carbon nanotubes with convective boundary conditions", *PloS one* 11(5), 152–923 (2016).
- [46] T. Abbas, M. Ayub, M.M. Bhatti, M.M. Rashidi, and M.E.S. Ali, "Entropy generation on nanofluid flow through a horizontal Riga plate", *Entropy* 18, 223 (2016).
- [47] G.H.R. Kefayati, "Simulation of double diffusive convection and entropy generation of power-law fluids in an inclined porous cavity with Soret and Dufour effects", *Int. J. Heat Mass Transfer* 94, 582–624 (2016).
- [48] T.Y. Na, *Computational Methods in Engineering Boundary Value Problem*, Academic Press, 71–76, 1979.